J|A|C|S
ARTICLES
Published on Web 01/14/2003

Ligand Exchange Dynamics in Aluminum Tris-(Quinoline-8-olate): A Solution State NMR Study

Marcel Utz,[†,‡] Changqing Chen,[†,§,||] Martha Morton,[||] and Fotios Papadimitrakopoulos[†,§,||]

Contribution from the Institute of Materials Science, the Department of Physics, the Department of Chemistry, and the Nanomaterials Optoelectronics Laboratory, University of Connecticut, Storrs, Connecticut 06269

Received July 23, 2002; E-mail: marcel.utz@uconn.edu

Abstract: The exchange kinetics between the three symmetry-inequivalent ligands in the meridianal isomer of aluminum tris-(quinoline-8-olate) (Alq_3), a widely used electron-transporting and light-emitting material in the field of organic light emitting diodes, have been studied using two-dimensional exchange NMR spectroscopy in solution. The three inequivalent ligands were found to exchange on a time scale of about 5 s^{-1} at room temperature. A simple first-order mechanism based on consecutive 180° flips of the ligands is sufficient to quantitatively explain the experimental data. Activation enthalpies between 83 and 106 kJ mol^{-1} were found for the flips of the three inequivalent ligands. The activation entropies are positive, suggesting a highly disordered transition state. These findings elucidate the internally mobile nature of the Alq_3 complex, and may have important implications for the morphology of vapor deposited thin films of Alq_3 as well as for crystallization-assisted device failures.

I. Introduction

Organic light emitting diode (OLED) devices have received considerable interest over the past fifteen years.[1] Aside from their low operational voltage, high brightness, efficiency, and tunable emission, their simple fabrication that is amenable to large area deposition renders them a formidable candidate for flat panel display applications. Aluminum tris-(quinoline-8-olate) (Alq_3) has been used as an electron transport and electron−hole recombination and emissive layer in the earliest working OLED devices,[2] and has remained a workhorse material for this purpose ever since. Alq_3 can be sublimed under mild conditions, which simplifies both purification and the deposition of thin films from the vapor phase. Its electron-transport capacity relies on the stability of its radical anion, which is not prone to oxidative attack by O_2.

A great deal of effort has been invested into optimization of Alq_3-based devices in terms of quantum efficiency and lifetime,[3−5] and the tuning of their luminescence color.[6,7] By contrast, most fundamental studies directed toward the properties of the Alq_3 molecule, its electronic structure,[8,9] dynamics,[12,11,10] and crystal polymorphs,[13,14] have only appeared recently.

The present work focuses on the internal dynamics of the Alq_3 molecule. Two-dimensional exchange NMR spectroscopy has been used in order to quantify the interchange of quinolinolate ligands in chloroform solution at various temperatures. Current OLED devices use Alq_3 in the form of amorphous thin films. Both the deposition of these films from the vapor phase and their gradual physical aging are kinetically controlled processes. Knowledge of the kinetic properties of the Alq_3 molecule constitutes an important step toward understanding both the processing and the long-time behavior of OLED devices. In particular, profound effects of the deposition rate and conditions on the performance of Alq_3-based devices have been demonstrated recently.[15−18]

[†] Institute of Materials Science, University of Connecticut.
[‡] Department of Physics, University of Connecticut.
[§] Department of Chemistry, University of Connecticut.
[||] Nanomaterials Optoelectronics Laboratory, University of Connecticut.

(1) Farchioni, R., Grosso, G., Eds. *Organic Electronic Materials*; Springer: Berlin, Heidelberg, 2001.
(2) Tang, C. W.; Van Slyke, S. A. *Appl. Phys. Lett.* **1987**, *51*, 913.
(3) Adachi, C.; Nagai, K.; Tamoto, N. *Appl. Phys. Lett.* **1995**, *66*, 2679−2681.
(4) Higginson, K. A.; Zhang, X.-M.; Papadimitrakopoulos, F. *Chem. Mater.* **1998**, *10*, 1017−1020.
(5) Papadimitrakopoulos, F.; Zhang, X.-M.; Thomsen III, D. L.; Higginson, K. A. *Chem. Mater.* **1996**, *8*, 1363−1365.
(6) Tang, C. W.; Van Slyke, S. A.; Chen, C. H. *J. Appl. Phys.* **1989**, *65*, 3610.
(7) Hopkins, T. A.; Meerholz, K.; Shaheen, S.; Anderson, M. L.; Schmidt, A.; Kippelen, B.; Padias, A. B.; Hall Jr., H. K.; Peyghambarian, N.; Armstrong, N. R. *Chem. Mater.* **1996**, *8*, 344−351.
(8) Curioni, A.; Boero, M.; Andreoni, W. *Chem. Phys. Lett.* **1998**, *294*, 263−271.
(9) Curioni, A.; Andreoni, W.; Treusch, R.; Himpsel, F. J.; Haskal, E.; Seidler, P.; Heske, C.; Kakar, S.; van Buuren, T.; Terminello, L. J. *Appl. Phys. Lett.* **1998**, *72*, 1575−1577.
(10) Esposti, A.; Brinkmann, M.; Ruani, G. *J. Chem. Phys.* **2002**, *116*, 798.
(11) Schmidbaur, H.; Lettenbauer, J.; Wilkinson, D. L.; Müller, G.; Kumberger, O. *Z. Naturforsch.* **1991**, *46b*, 901−911.
(12) Baker, B. C.; Sawyer, D. T. *J. Am. Chem. Soc.* **1968**, *40*, 1945−1951.
(13) Brinkmann, M.; Gadret, G.; Muccini, M.; Taliani, C.; Masciocchi, N.; Sironi, A. *J. Am. Chem. Soc.* **2000**, *122*, 5147−5157.
(14) Braun, M.; Gmeiner, J.; Tzolov, M.; Coelle, M.; Meyer, F. D.; Milius, W.; Hillebrecht, H.; Wendland, O.; von Schütz, J. U.; Brütting, W. *J. Chem. Phys.* **2001**, *114*, 9625−9632.
(15) Cheng, L. F.; Liao, L. S.; Lai, W. Y.; Sun, X. H.; Wong, N. B.; Lee, C. S.; Lee, S. T. *Chem. Phys. Lett.* **2000**, *319*, 418−422.
(16) Kim, S. Y.; Ryu, S. Y.; Choi, J. M.; Kang, S. J.; Park, S. P.; Im, S.; Whang, C. N.; Choi, D. S. *Thin Solid Films* **2001**, *398−399*, 78−81.
(17) Qin, D. S.; Li, D. C.; Wang, Y.; Zhang, J. D.; Xie, Z. Y.; Wang, G.; Wang, L. X. *Appl. Phys. Lett.* **2001**, *78*, 437−439.
(18) Chen, B. J.; Lai, W. Y.; Gao, Z. Q.; Lee, C. S.; Lee, S. T.; Gambling, W. A. *Appl. Phys. Lett.* **1999**, *75*, 4010−4012.

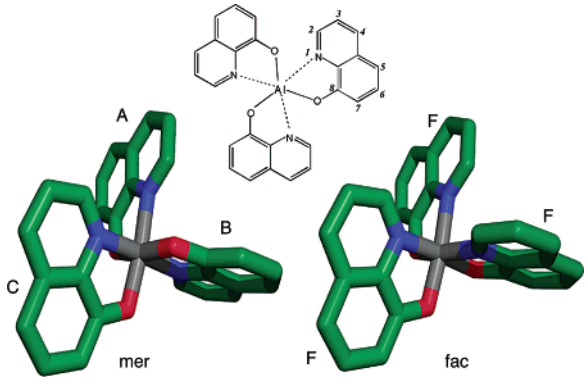

Figure 1. Structure (top) and 3D rendering of the meridianal (left) and facial (right) isomers of Alq_3. Atomic positions for *mer*-Alq_3 have been taken from ref 11; the nomenclature of the ligands follows ref 12 . In the meridianal isomer, the ligands are readily identified by the atoms that occupy opposite positions on the coordination octahedron. For A, these are both oxygens; for B, nitrogens; and for C, one oxygen and one nitrogen. In the facial isomer, opposite corners of the octahedron are occupied by one oxygen and one nitrogen, respectively.

Alq_3 is an octahedrally coordinated chelate complex, with the aluminum ion surrounded by three identical quinolinolate anions. In principle, both a meridianal isomer, with the oxygen atoms forming a meridian of the distorted coordination octahedron, and a facial isomer, with the oxygens forming a face of the octahedron, could exist. In the facial isomer, the three ligands are equivalent by symmetry, whereas in the meridianal isomer, they are distinct (cf. Figure 1). As is well-known from earlier NMR studies,[11] as well as from X-ray diffraction,[11,13] the meridianal isomer is the stable form at room temperature. Density functional calculations have yielded an energy difference of about 20 kJ/mol between the two isomers,[8] corresponding to a Boltzmann factor of about 10^{-4} at room temperature. Although earlier X-ray diffraction studies have focused on solvated forms of Alq_3,[11] several crystalline polymorphs of pure Alq_3 have been characterized by powder and single-crystal X-ray diffraction more recently.[13,14] α-Alq_3 and β-Alq_3 are obtained simultaneously by slow vapor deposition under N_2 and by recrystallization from acetone at room temperature.[13] A disordered high-temperature variant of the α form, γ-Alq_3, has also been observed.[13] All of these phases contain a racemic mixture of the two enantiomers of the meridianal form of Alq_3. Recently, a fourth crystalline phase (δ) resulting from vapor deposition at high substrate temperature was reported and tentatively attributed to the facial isomer.[14]

The absence of an axis of symmetry in the meridianal form of Alq_3 leads to the three quinolinolate ligands being distinguishable. Their inequivalence becomes immediately apparent in the proton NMR spectrum in solution,[11,12] where a separate set of resonances can be observed for each of the three ligands. In particular, the protons on the pyridyl side of the quinoline unit are well resolved. It has been shown that the line shape of the proton resonances strongly depends on temperature, suggesting exchange dynamics between the ligands.[11] A similar conclusion was drawn as early as 1968 by Baker and Sawyer,[12] who observed that the spectral lines of equivalent protons on different ligands collapsed to their average positions at 116 °C. However, the precise nature of the exchange processes has not been investigated further. Two-dimensional NMR exchange spectroscopy[19] is an ideal tool for the quantification of chemical

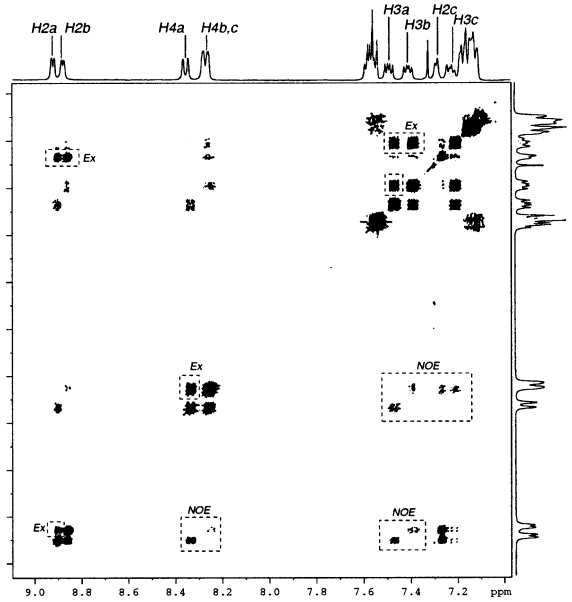

Figure 2. Two-dimensional exchange NMR spectrum of Alq_3 in $CDCl_3$ solution at 300 K and a mixing time of $\tau_m = 200$ ms. Cross-peaks of two different types appear: Exchange peaks appear with positive sign between corresponding protons on different ligands (Ex), whereas NOE peaks between different protons on the same ligand appear with negative sign (NOE).

exchange processes, provided that the exchanging species are clearly resolved in the NMR spectrum, and the time scale of the process is shorter than the spin−lattice relaxation time. Both conditions are almost ideally met by Alq_3 in $CDCl_3$ solution.

II. Materials and Methods

Alq_3 has been synthesized as described elsewhere,[5] and was purified by sublimation. The material was then dissolved at a concentration of 13 mg/ml in anhydrous $CDCl_3$ (Aldrich) which was previously dried over molecular sieves for 48h. The solution was transferred into a J-Young NMR tube equipped with a Teflon valve. All operations were carried out under anhydrous nitrogen atmosphere in a glovebox.

NMR spectra were acquired on a Bruker DRX spectrometer operating at a proton Larmor frequency of 400 MHz. 2D exchange spectra were recorded using a three-pulse NOESY sequence, with a 90° pulse duration of 6.5 μs. The spectral width in both dimensions was 3 ppm. 280 t_1 increments, with 16 scans each, were recorded with a recycle delay of 1.5 s. The T_1 (spin−lattice) relaxation times of the different protons were measured independently using the inversion−recovery method. The spectra were processed and peak intensities were obtained with the help of Bruker software.

III. Results and Discussion

A. Ligand Assignment of the ^{1}H Spectrum. The one-dimensional proton solution NMR spectrum of Alq_3 at room temperature in $CDCl_3$ is shown at the top of Figure 2. The protons on the pyridyl side of the quinolinolate unit (H2, H3, and H4) are the most well resolved. The ligand assignments indicated in the figure have been obtained from the double quantum-filtered COSY spectrum (not shown). Correlation spectroscopy only leads to grouping of the resonances per ligand, and does not reveal which group is associated with which of the three inequivalent ligands in the meridianal isomer. However, Baker and Sawyer have predicted the chemical shifts of

(19) Jeener, J.; Meier, B. H.; Bachmann, T.; Ernst, R. R. *J. Chem. Phys.* **1979**, *71*, 4546.

all protons in meridianal Alq_3 from the spectra of 8-hydroxy quinoline in acidic and basic conditions and the ring current effects to be expected from the geometry of *mer*-Alq_3.[12] The grouping given by Baker and Sawyer is consistent with our double quantum filtered COSY results, and we have adopted their group ligand assignment and nomenclature.

B. Ligand Exchange Kinetics. The two-dimensional exchange spectrum of Alq_3 in $CDCl_3$ solution at a temperature of 310 K and a mixing time of $\tau_m = 200$ms is shown in Figure 2. The spectrum exhibits off-diagonal peaks of two different kinds. There are positive cross-peaks between protons of the same type on different ligands (inter-ligand peaks), and negative signals between protons of different type on the same ligand (intra-ligand peaks). While the former are indicative of ligand exchange, the latter are caused by the Nuclear Overhauser effect, and are not of interest in the present context. The exchange cross-peaks of both the H2 and the H3 protons are fully resolved. In the case of H4, two of the three ligands have almost the same chemical shift, leading to overlap of the cross-peaks. The H2 and H3 peaks were therefore selected for analysis of the exchange kinetics. Under the conditions of Figure 2, the exchange is nearly complete, and the cross-peaks have the same intensity as the diagonal peaks. At 283 K, however, the exchange was found to be much slower, reaching less than 10% at the same mixing time of $\tau_m = 200$ms. At all temperatures studied, the three different types of exchange cross-peaks (AB, AC, and BC) exhibit clearly different time dependencies. This indicates that the exchange occurs by some specific mechanism, rather than by complete destruction and re-formation of the entire organometallic complex.

To establish the first-order character of the exchange process, the concentration dependence of the 2D exchange spectra has been studied. We found no change in the relative cross-peak intensities upon changing the Alq_3 concentration from 13 mg/ml to 6.5 mg/ml at a temperature of 300 K and a mixing time of 200 ms. Under these conditions, the exchange is about 50% complete, and a substantial change in the rate constants would immediately be reflected in the cross-peak intensities. We therefore conclude that the exchange process follows first-order kinetics.

C. Kinetic Model and Activation Parameters. A first-order kinetic model of the exchange mechanism was constructed based on the ligand-flip mechanism proposed by Schmidbaur et al.[11] The basic step consists of breaking an Al−N bond, creating a ligand that is free to rotate around the Al−O bond. The partially bonded ligand can then reconnect either in the same orientation, or rotated by 180° after overcoming a rotational energy barrier. Such inversions cause different rearrangements of the ligands, depending on which one is flipped.

Flipping any of the ligands in the facial isomer converts the molecule to the meridianal form, where the flipped ligand acquires "B" identity, and the other two become A and C, respectively. Correspondingly, a flip of the B ligand in the meridianal isomer converts to the facial form, equalizing the three ligands through the 3-fold symmetry axis. Flipping either A or C in the meridianal isomer interchanges the two other ligands, whereas the active quinolinolate moiety retains its identity, as illustrated in Figure 4. The figure in the table of contents of this issue shows a flip of B, leading to the facial isomer.

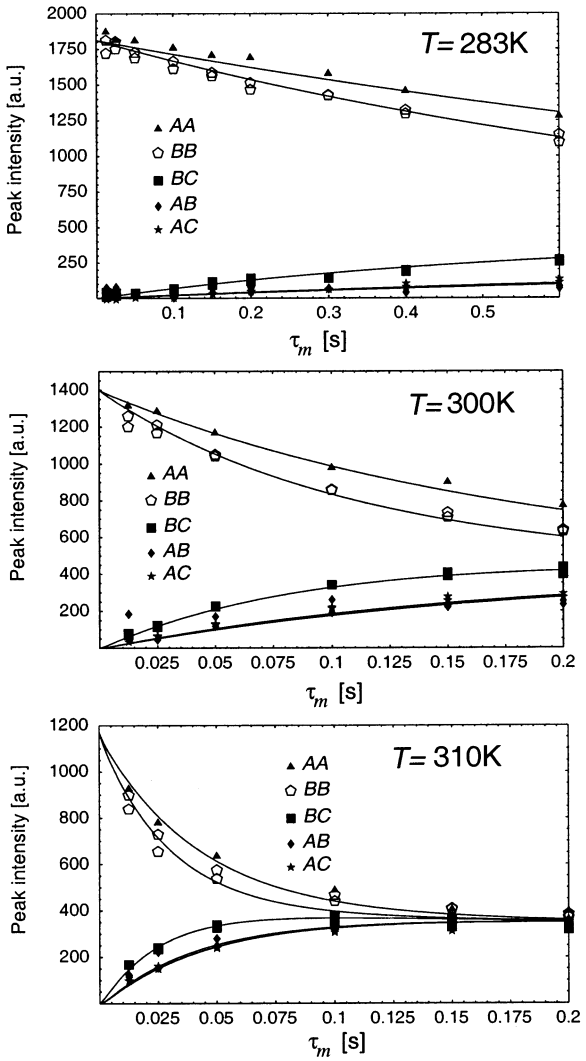

Figure 3. Integrated peak intensities as a function of mixing time at three different temperatures. Data for both H2 and H3 are shown. The solid lines represent the first-order kinetic model described in the text. Note the different horizontal scale in the top panel ($T = 283$ K).

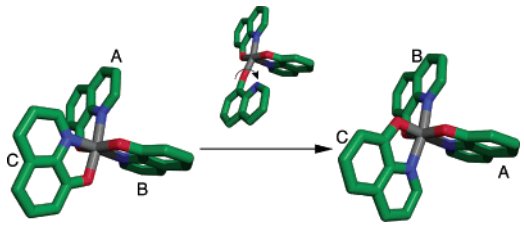

Figure 4. Schematic representation of the elementary mechanism of exchange that forms the basis of the first-order kinetic model. Breaking the N−Al bond of the C-ligand in *mer*-Alq_3 allows it to rotate by 180° about the Al−O bond. This rotation leads to an interchange of A and B, whereas the rotating ligand C retains its identity.

Both the facial and the meridianal isomer of Alq_3 are chiral. The flip mechanism outlined above preserves the sense of chirality. In the present context, because the enantiomers are not distinguished in the NMR spectrum, a perfectly racemic mixture can be assumed, and it is sufficient to discuss only one of the enantiomers.

The complete exchange model can therefore be formulated in terms of four independent reactions

$$\mathrm{ABC} \xrightarrow[k_1]{} \mathrm{ACB}$$

$$\mathrm{ABC} \xrightarrow[k_2]{} \mathrm{BAC}$$

$$\mathrm{ABC} \xrightarrow[k_3]{} \mathrm{FFF}$$

$$\mathrm{FFF} \xrightarrow[k_4]{} \mathrm{ABC, ACB,...} \quad (1)$$

where ABC etc. stands for different permutations of the meridianal and FFF for the facial isomer. With regard to the last reaction in eq 1, it has to be taken into account that its result can be any permutation of the ligands with equal probability, since they are equivalent by symmetry in the facial isomer. The complete reaction network comprises six distinguishable permutations for the meridianal and one for the facial isomer. The reaction network can be described by a 7×7 kinetic matrix

$$\mathbf{K} = \begin{bmatrix} -\Sigma & k_2 & 0 & 0 & 0 & k_1 & k_4 \\ k_2 & -\Sigma & k_1 & 0 & 0 & 0 & k_4 \\ 0 & k_1 & -\Sigma & k_2 & 0 & 0 & k_4 \\ 0 & 0 & k_2 & -\Sigma & k_1 & 0 & k_4 \\ 0 & 0 & 0 & k_1 & -\Sigma & k_2 & k_4 \\ k_1 & 0 & 0 & 0 & k_2 & -\Sigma & k_4 \\ k_3 & k_3 & k_3 & k_3 & k_3 & k_3 & -6k_4 \end{bmatrix} \quad (2)$$

where $\Sigma = k_1 + k_2 + k_3$. The exchange process is then described by the coupled first-order differential equations

$$\frac{d}{dt}\mathbf{c} = \mathbf{K}\mathbf{c} \quad (3)$$

where the elements of the vector **c** denote, sequentially, the concentrations of the permutations ABC, BAC, BCA, CBA, CAB, ACB, and FFF. The contributions of the exchange between two of the above species k and l to the exchange NMR spectrum is proportional to[20]

$$a_{kl} = \exp\left(\tau_m\left(\mathbf{K} - \frac{1}{T_1}\mathbf{I}\right)\right)_{kl} c_l \quad (4)$$

with the mixing time τ_m, and the spin−lattice relaxation time T_1. **I** represents the identity matrix. In the NMR spectrum, the three different *ligands* in the meridianal isomer, rather than the six different *permutations* are resolved. The facial isomer would give rise to a single set of resonances, if it were present in detectable concentration. To correctly account for multistep exchange, however, it is necessary to formulate the exchange problem in terms of all possible permutations. The peak intensities in the exchange NMR spectrum can be calculated by adding the exchange coefficients a_{kl} appropriately. For example, the coefficient a_{12}, linking the permutations ABC and BAC, contributes to the exchange peak between ligands A and B, and to the diagonal peak of ligand C.

The integrated peak intensities of the H2 and the H3 protons as a function of mixing time τ_m at three different temperatures are shown in Figure 3. The symbols represent experimental values; the lines indicate the best fit of the data according to the above first-order kinetic model. Values for the reaction rates k_1, k_2, and k_3 have been obtained by least-squares fitting of the above model to the experimental data. The value for k_4 was kept fixed at 100 s^{-1}. The concentration of the facial isomer is essentially given by the ratio k_3/k_4. Because the presence of the facial isomer cannot be detected in the NMR spectra, this ratio must be lower than 10^{-2}. The observable peak intensities of the meridianal isomer are insensitive to the value of k_4, provided it is large. The T_1 relaxation times, which are also taken into account in the model, have been determined independently for each resonance line using the inversion recovery method.

Table 1. Rate Constants Determined by Least-Squares Fitting of the Experimental H2 and H3 Peak Intensities[a]

T/K	k_1/s^{-1}	k_2/s^{-1}	k_3/s^{-1}
283	0.29 ± 0.75	0.00 ± 1.00	0.39 ± 0.75
300	2.35 ± 0.60	0.14 ± 0.60	4.99 ± 0.60
310	6.68 ± 3.00	0.65 ± 6.00	22.01 ± 3.00

[a] Error margins represent individual 95% confidence intervals.

Figure 3 summarizes the experimental data at the three temperatures investigated, 283, 300, and 310 K. The first-order model is capable of fitting the data to within experimental error at each temperature. The values of the three reaction constants k_1, k_2, and k_3 resulting from the fitting procedure are given in Table 1. The fit is numerically quite robust, with an almost spherical 95% confidence contour in the parameter space (not shown). Whereas both k_1 and k_3 are quite narrowly constrained by the fit, the error margins for k_2 are relatively wide. All reaction rates are very temperature sensitive, changing by up to a factor of 50 as the temperature is raised from 283 to 310 K.

Because it is not unconceivable that the exchange reactions are catalyzed by traces of moisture, the rate constants were also measured with a sample to which 15 ppm of H_2O had been added. No significant change in the exchange rates over the results stated in Table 1 was detected. It therefore seems that water does not play a major role in the ligand exchange process. This finding is consistent with the proposed exchange mechanism, which is based on spontaneous breaking of the Al−N bond, whereas H_2O attacks Alq_3 by hydrolysis of the Al−O bond.[5]

Because the reaction rate constants have been determined at different temperatures, it is possible to estimate the activation parameters following Eyring's law

$$k = \frac{k_b T}{h} \exp\frac{\Delta S}{k_b} \exp -\frac{\Delta H}{k_b T}$$

where ΔS and ΔH represent the activation entropy and enthalpy, and k_b denotes Boltzmann's constant. An Eyring plot of the data is shown in Figure 5. All three reaction rates' temperature dependences are accurately represented by straight lines. This suggests that the three rate constants have a real physical meaning rather than just being fit parameters, thus adding to the credibility of the proposed mechanism of ligand exchange. Due to the smallness of the reaction rates k_2, the associated error margins are large. This leads to a very poor quality of regression for this reaction, and the activation parameters cannot be reliably determined. In the following, we therefore restrict our discussion to the activation parameters of k_1 and k_3.

The activation parameters determined from the Eyring plot are given in Table 2, with error margins reflecting the uncertainties in the individual rate constants. The activation enthalpies

(20) Ernst, R. R.; Bodenhausen, G.; Wokaun, A. *Principles of Nuclear Magnetic Resonance in One and Two Dimensions*, Clarendon Press: Oxford, 1987.

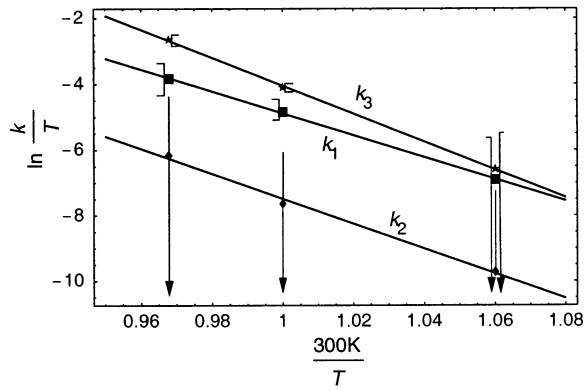

Figure 5. Eyring plot of the rate constants determined by fitting the rate constants k_1, k_2, and k_3 to the experimental data at three different temperatures.

Table 2. Activation Parameters Obtained from Eyring Analysis of the Rate Constants Given in Table 1[a]

	k_1	k_2	k_3
ΔH/(kJ/mol)	85.5 ± 8.1	53.2 ± 24.0	105.3 ± 3.8
ΔS/(J/molK)	93.5 ± 27.4	−23.5 ± 47.8	167.7 ± 13.0

[a] The indicated standard errors of regression take into account the error margins of the individual rate constants.

ΔH are of the order of 90 kJ/mol. These rather large values would render ligand exchange in Alq_3 an exceedingly slow process at room temperature, if it were not for the large, positive activation entropies ΔS. As mentioned in the Introduction, the difference in energy between the meridianal and the facial isomer of Alq_3 has been determined by numerical simulation at about 20 kJ/mol. In light of the proposed reaction mechanism, the activation barriers should be substantially higher than this difference because one coordination bond is broken in the transition states. The activation enthalpies reported here are consistent with this expectation. It would be very interesting to compare our values to quantum chemical calculations of the transition states. To our knowledge, no such data has been reported to date.

Because breaking a coordination bond leads to a state of higher disorder, the fact that the activation entropies are positive is consistent with the proposed reaction mechanism. It is interesting to note that the activation entropy for k_3, which leads to the 3-fold degenerate facial state, is significantly larger than that for k_1, which links nondegenerate states.

The exchange processes in Alq_3 may have important practical implications. It has been shown that the conditions under which amorphous Alq_3 films are deposited crucially influence device performance. Chen et al.[18] have demonstrated that the carrier mobility in Alq_3 films increases by 2 orders of magnitude as the deposition rate is reduced from 0.7 nms^{-1} to 0.2 nms^{-1}. Because the diameter of a single Alq_3 molecule is roughly 1 nm, these deposition rates approximately correspond to 0.7 and 0.2 monolayers per second, respectively. This time scale is comparable to the rates of ligand exchange reported here. A similar effect has been reported by Qin et al.[17] with respect to the substrate temperature.

Alq_3 is a bulky molecule, which leads to strong kinetic hindrance of its crystallization. It is therefore to be expected that the quality of amorphous packings is strongly affected by the deposition rate. If the time for the deposition of a monolayer is much longer than the time scale of internal mobility of Alq_3, then each incoming molecule can "adapt" to some extent to the growing amorphous surface. This leads to a dense packing with a high degree of short-range order. Deposition at substantially faster rates, in contrast, would be expected to lead to a more disordered amorphous packing.

Although the coincidence of time scales is suggestive, it does not prove that the packing geometry in Alq_3 thin films is affected by the deposition rate and substrate temperature. In a similar way, it is unclear how much of the internal mobility of Alq_3 in solution survives in the amorphous solid state. This information would be very interesting in view of physical aging and gradual device failure.[4] Solid-state NMR studies that will clarify these issues are currently underway in our laboratory, and will be reported at a later occasion.

Conclusions

The kinetics of exchange between the inequivalent ligands in the meridianal isomer of Alq_3 have been studied at different temperatures by 2D exchange proton NMR spectroscopy. The ligands were found to exchange on a time scale of about $5s^{-1}$ at room temperature. The observed exchange pattern can be explained quantitatively by a simple first-order mechanism based on 180° flips of the ligands with four independent reaction rates. Three of these, the flip rates of the ligands in the meridianal isomer, can be determined experimentally, whereas the flip rate of the ligands in the facial isomer is too large to be quantified. The activation enthalpies of the flip rates in the meridianal isomer range from 53 to 105 kJ mol^{-1}, leading to a very strong temperature dependence of the exchange process. The activation entropies of two out of the three reactions were found to be large and positive, suggesting a highly disordered transition state.

Acknowledgment. Parts of the present work have been supported by the National Science Foundation through CAREER awards to both M.U. (DMR-0094290) and F.P. (DMR-970220), as well as by a type G grant from the Petroleum Research Fund to M.U. F.P. also gratefully acknowledges support of the Critical Technologies Program by Connecticut Innovations, Inc., and Trans-Lux Corp.

JA027825O